Optical Pumping

Idrees Al-Khalidi

Revision: 23 May 2024

1 Abstract

In the "Optical Pumping" experiment, polarized light is used to excite Rubidium atoms, which appear as two isotopes in this experiment: ^{85}Rb and ^{87}Rb (University of California, Berkeley). The difference between energy levels is observed, as well as the effect of radio-frequency magnetic field on the polarization of Rubidium atoms. Thus, the nuclear spin and the strength of Earth's magnetic field can be determined. In this experiment, I_{85} is calculated to be 2.548 ± 0.00351 and I_{87} is calculated to be 1.531 ± 0.00251. Additionally, the strength of Earth's magnetic field is calculated to be 0.428 G ± 0.00222 G.

2 Introduction

This experiment highlights the use of quantum states to describe the movement of electrons and nuclei in atoms (1). To measure the energy of quantum states, the difference in energy between energy levels is taken into account. The splitting of energy levels due to angular momentum and a magnetic field is also measured.

3 Background Research and Theory

3.1 Energy Level Splitting in Rubidium

Rubidium, an element with an atomic number of 87, appears as the isotopes ^{85}Rb and ^{87}Rb in this experiment (1). There is one valence electron in the electronic ground state of Rubidium that is located in the 5s atomic orbital. The nearest orbital, the 5p orbital, is 1.6 eV above the 5s orbital and is where the valence electron is located in the first excited state of Rubidium.

There are 3 values of angular momentum (1). The first value of angular momentum, "L", describes the electron orbital angular momentum. The second value of angular momentum, "S", describes the electron spin. The third value of angular momentum, "I", describes the nuclear spin.

In the electronic ground state of Rubidium, L = 0 and S = 1/2 (1). In the first excited state of Rubidium, L = 1 and S = 1/2. For ^{85}Rb, I = 5/2. For ^{87}Rb, I = 3/2. As a result, there are more angular momentum states in the 5s ground state and the 5p excited state. In the 5s ground state, there are (2S + 1) * (2I + 1) states. In the 5p excited state, (2L + 1) * (2S + 1) * (2I + 1) states.

The first splitting of the energy levels is fine energy splitting that is caused by the net effect of electron orbital angular momentum, L, and electron spin, S (1). The notation of the new states is $^{2S+1}L_J$ The 5p excited state splits into $^2P_{1/2}$ and $^2P_{3/2}$. The 5s electronic state does not split, but instead becomes $^2S_{1/2}$. Wavelengths of 795 nm and 780 nm are needed for electrons to transfer from the ground state to states in $^2P_{1/2}$ and $^2P_{3/2}$, respectively. The total electronic angular momentum, $\vec{J}$, of energy eigenstates for energy levels in fine energy splitting is given by Equation 1:

$$\vec{J} = \vec{L} + \vec{S} \tag{1}$$

The second splitting of the energy levels is hyperfine splitting, which is caused by the net effect of the electron orbital angular momentum, L, and nuclear

spin, I. The total angular momentum, $\vec{F}$, of energy eigenstates for energy levels in the hyperfine structure is given by Equation 2:

$$\vec{F} = \vec{I} + \vec{J} \tag{2}$$

The third splitting of the energy levels is caused by magnetic fields. For example, for ^{87}Rb, the basis states $|J, I, m_J, m_I\rangle$ span the ground state. The values of m_J and m_I are given by Equations 3 and 4, respectively.

$$m_J \in \{-1/2, 1/2\} \tag{3}$$

$$m_I \in \{-3/2, -1/2, 1/2, 3/2\} \tag{4}$$

The Hamiltonian for the hyperfine structure is given by Equation 5, in which $\vec{\mu_J}$ and $\vec{\mu_I}$ are the magnetic dipole moments of electrons and nuclei, respectively (1).

$$H_{hfs} = -\vec{\mu_I} \cdot (\vec{B_J} + \vec{B_{ext}}) - m\vec{u}_J \cdot \vec{B_{ext}} \tag{5}$$

The derivations for $\vec{\mu_J}$ and $\vec{\mu_I}$ are given in Equations 6-9.

$$\vec{\mu_J} = g_J \mu_B J \tag{6}$$

$$\mu_B = \frac{e\hbar}{2m_e} \tag{7}$$

$$\vec{\mu_I} = g_I \mu_N \vec{I} \tag{8}$$

$$\mu_N = \frac{e\hbar}{2m_p} \tag{9}$$

Additionally, the relationship between the frequency related to the energy splitting and the applied magnetic field is given by Equation 10 (1).

$$\frac{\nu}{B_{exp}} = \frac{2.799}{2I+1} \frac{MHz}{G} \tag{10}$$

Furthermore, the energy splitting of ^{85}Rb and ^{87}Rb is shown in Figures 1 and 2 (MIT Department of Physics 2011)

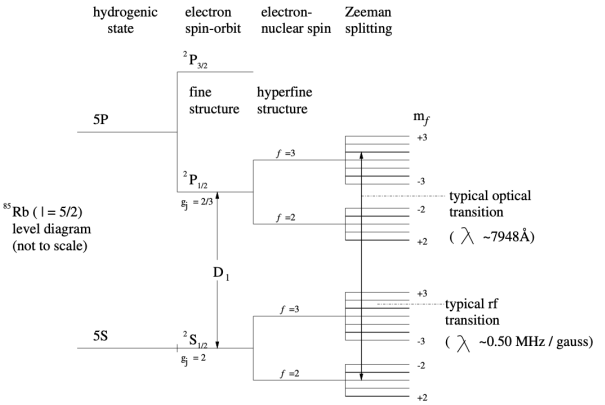

Figure 1: Figure 1 from the reading "Optical Pumping" by the MIT Department of Physics depicting energy level splittings for ^{85}Rb that are not to scale (2).

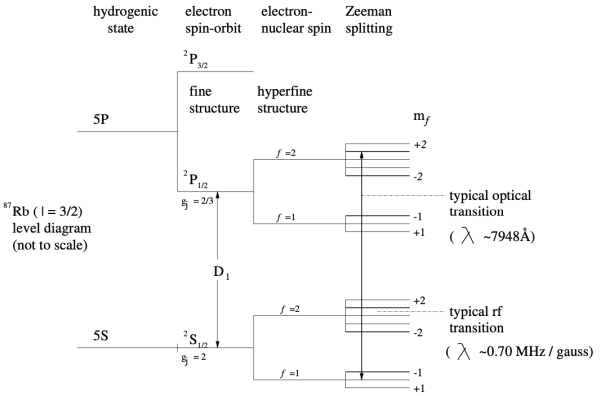

Figure 2: Figure 2 from the reading "Optical Pumping" by the MIT Department of Physics depicting energy level splittings for ^{87}Rb that are not to scale (2).

3.2 Optical Pumping

The frequency ν is used to cause rubidium atoms to be in a final state $|F, m_F \pm 1\rangle$ from an initial state $|F, m_F\rangle$ (1). To account for the number of atoms that undergo this change in hyperfine states, the atoms

must initially be spin polarized to allow for radio-frequency magnetic field to cause atoms to undergo this transition. Additionally, Equation 7 describes the probabilities P_1 and P_2 that an atom will have an energy of E_1 and E_2, respectively, at temperature T.

$$\frac{P_2}{P_1} = \exp(-\frac{E_2 - E_1}{k_B T}) \tag{11}$$

To spin-polarize the atoms, circularly-polarized infared light is used to excite atoms and causes Δm_F to be equal to {-1, 0, +1} for emission and equal to {+1} for absorption, which is described in Figure 3 (1; University of Wisconsin-Madison 2019).

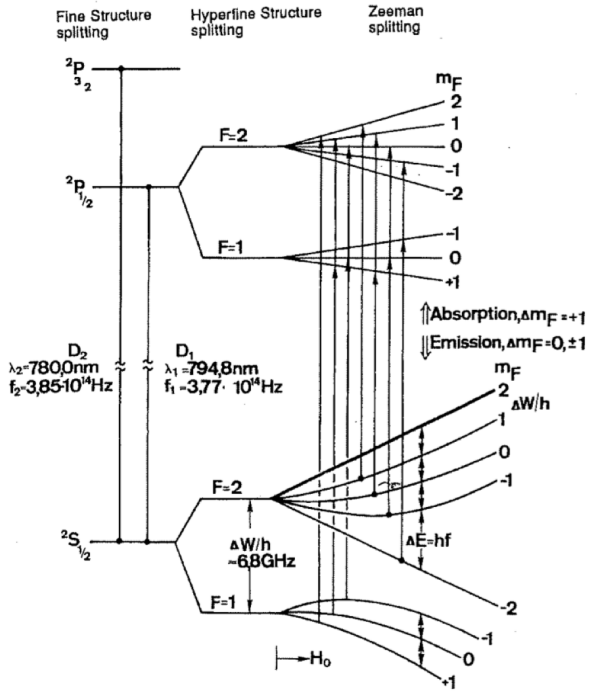

Figure 3: Figure 1 from the reading "Optical Pumping of Rubidium" by the University of Wisconsin-Madison that depicts the optical transitions in ^{87}Rb (4)

3.3 Magnetic Resonance

Because the atoms eventually reach a pumped state, light is no longer absorbed and the state is referred to as a "dark state" (1). Thus, applying a resonant radio-frequency magnetic field causes the atoms to exit from the "pumped state" and absorb light again, causing the light level to decrease in the photodetector in a process known as "optically detected magnetic resonance".

4 Methods

To determine the temperature at which there was most peak in the ODMR signals for ^{85}Rb and ^{87}Rb, measurements of the peaks in ODMR signals for both isotopes were taken for various temperatures and the temperature range that caused the highest peaks in signals was used throughout the experiment (1).

3 trials to detect the resonance frequency for ^{85}Rb and ^{87}Rb were taken to measure the uncertainty in resonance frequency for both isotopes (1). For both isotopes, various values of current were used with "forward" and "reverse" coil polarity. The values of the current ranged from 0.90 A to 1.15 A. Additionally, measurements of the resonance frequency at 0 current were taken. Also, with the rf modulation turned off, which causes there to be no external magnetic field, the resonance frequency is measured. Lastly, the "pumping time" and "relaxation time" were measured by measuring the time-trace of the photodiode signal.

5 Experimental Design

In this experiment, a bulb is heated so that rubidium that is on the walls of the bulb is emitted into the buffer gas (1). Also, a lamp that holds ground state rubidium releases light that is polarized by entering an optical polarizer and a "D1 pass filter" that exclusively allows light with a wavelength of approximately 795 nm to pass through. Furthermore, the radio-frequency magnetic field is produced by a sinusoidal current that is generated by the SRS DS345 function generator that has current passing through rf coils

to induce Zeeman splitting transitions. A light-proof and insulated box contains the bulb, heater, and coils allows for measurements to be taken for a longer period of time. The magnetic field created by the sinusoidal current is given by Equation 12, in which "N" is equal to the number of turns for the coils, "i" is the current used, and "a" is equal to the radius of the coils. Additionally, the voltage through the shunt resistor is equal to 10 mV for every ampere of current.

$$0.9 * 10^{-2} \frac{Ni}{a} * \frac{Gm}{A} \tag{12}$$

To test for detection of ODMR signals, a sinusoidal current is generated with the SRS DS345 and a frequency of the magnetic field and the photodiode signal are detected, resulting in two peaks, similar to Figure 5, which is in the Laboratory Manual for this experiment.

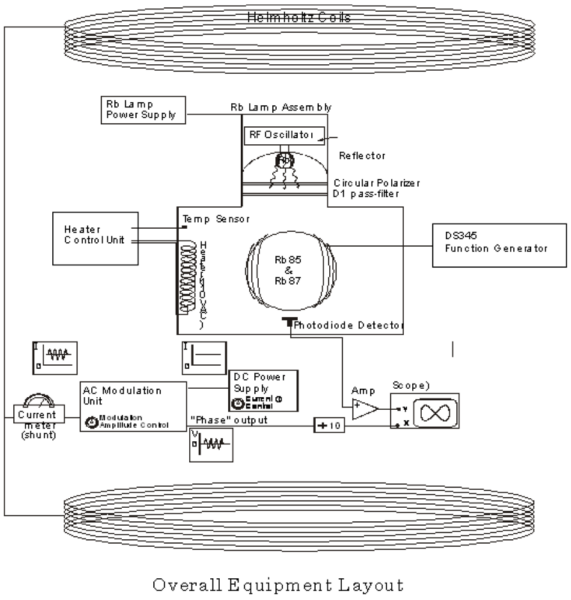

Figure 4: Figure 4 from the Laboratory Manual for this experiment (1). This figure depicts the equipment used in the experiment (1).

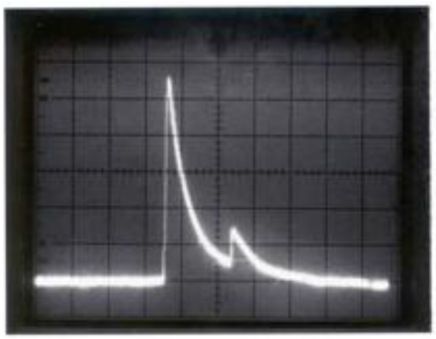

Figure 5: Figure 7 from the Laboratory Manual for this experiment, which shows the shape of the ODMR signals that are detected (1)

After, the temperature range that results in the highest peaks for ODMR signals, is found. In the case of this experiment, the temperature range was 38 °C to 44 °C. Additionally, current was adjusted from 0.90 A to 1.14 A for forward and reverse "coil polarity" while the resonance frequency was being monitored for both isotopes. Additionally, with the current at 0 A, the resonance frequency was measured for both isotopes. Both resonance frequencies were identified for each isotope by detecting which resonance frequency was greater than the other resonance frequency, due to ^{87}Rb having a higher resonance frequency than ^{85}Rb. In addition, the current at which a resonance occurred while the rf modulation was disabled was found. Lastly, the "pumping time" and "relaxation time" were found by using the SRS DS345 to modulate a sinusoidal signal by a square wave and monitoring the rise and fall of the photodiode signal.

6 Raw Data

6.5) T (°C) | ^{85}Rb Peak | ^{87}Rb Peak | Scale

46.0	108 ✓	35 ✓	0.1 V
45.5	110	36	0.1 V
45	112	35	0.1 V
44.5	115	35	0.1 V
44.0	115	32	0.1 V
43.5	118	33	0.1 V
43.0	118	30	0.1 V
42.5	118	28	0.1 V
42.0	115	25	0.1 V
41.5	115	25	0.1 V
41.0	110	24	0.1 V
40.5	109	23	0.1 V
40.0	105	22	0.1 V
39.5	104	20	0.1 V
39.0	100	19	0.1 V
38.5	98	18	0.1 V
38.0	95	18	0.1 V
37.5	91	19	0.1 V
37.0	90	15	0.1 V
36.5	87	14	0.1 V
36.0	85	12	0.1 V

Figure 6: A data table to detect the highest peak in ODMR signals for ^{85}Rb and ^{87}Rb.

6.4) Uncertainty measurement

T (°C)	ν for ^{85}Rb	Current	Rubidium Lamp Output Current	Multimeter Voltage	Field Modulation
39.3	2,221,500,000 Hz	1.00 A	23.5 mA	10.257 mV	5
42.2	2,221,730,000 Hz	1.00 A	23.5 mA	10.257 mV	5
46.6	2,221,440,000 Hz	1.00 A	23.6 mA	10.257 mV	5

Uncertainty measurement

T (°C)	ν for ^{87}Rb	Current	Rubidium Lamp Output Current	Multimeter Voltage	Field Modulation
39.1	3,406,000,000 Hz	1.00 A	25 mA	10.260 mV	7
38.3	3,408,050,000 Hz	1.00 A	25 mA	10.262 mV	7
42.6	3,410,000,000 Hz	1.00 A	25 mA	10.262 mV	7

Figure 7: Data tables to detect the uncertainty in the resonance frequencies for ^{85}Rb and ^{87}Rb.

^{85}Rb Current	"Coil Polarity"	Resonance Frequency	Multimeter Voltage	T (°C)	Field Modulation
1.05 A	Forward	2,394,000.000 Hz	10.960 mV	40.0 °C	S
1.05 A	Reverse	1,968,600.000 Hz	-10.765 mV	38.1 °C	S
1.10 A	Reverse	2,089,600.000 Hz	-11.383 mV	41.1 °C	S
1.15 A	Reverse	2,186,500.000 Hz	-11.895 mV	40.6 °C	S
1.13 A	Reverse	2,152,200.000 Hz	-11.576 mV	38.9 °C	S
0.95 A	Reverse	1,935,500.000 Hz	-09.756 mV	42.3 °C	S
0.90 A	Reverse	1,685,700.000 Hz	-09.959 mV	41.3 °C	S
0.90 A	Forward	2,069,000.000 Hz	09.254 mV	39.7 °C	S
0.95 A	Forward	2,164,300.000 mV	09.731 mV	39.0 °C	S
1.00 A	Forward	2,264,300.000 mV	10.221 mV	40.5 °C	S
1.10 A	Forward	2,476,000.000 mV	11.269 mV	40.0 °C	S
1.15 A	Forward	2,585,500.000 mV	11.798 mV	39.3 °C	S

Figure 8: A data table to detect the resonance frequencies for ^{85}Rb using various values of current.

^{87}Rb Current	"Coil Polarity"	Resonance Frequency	Multimeter Voltage	T (°C)	Field Modulation
1.15 A	Forward	5,326,000.000 Hz	11.773 mV	41.2 °C	S
1.10 A	Forward	5,221,000.000 Hz	11.273 mV	40.7 °C	S
1.05 A	Forward	5,122,000.000 Hz	10.786 mV	40.2 °C	S
1.00 A	Forward	5,410,000.000 Hz	10.2558 mV	39.5 °C	S
0.95 A	Forward	5,247,000.000 Hz	09.7418 mV	39.0 °C	S
0.90 A	Forward	5,102,000.000 Hz	09.245 mV	38.6 °C	S
1.15 A	Reverse	5,289,000.000 Hz	-11.748 mV	42.4 °C	S
1.10 A	Reverse	5,102,000.000 Hz	-11.236 mV	41.6 °C	S
1.05 A	Reverse	2,980,000.000 Hz	-10.767 mV	40.8 °C	S
1.00 A	Reverse	2,819,000.000 Hz	-10.236 mV	40.4 °C	
0.95 A	Reverse	2,695,000.000 Hz	-09.769 mV	39.9 °C	S
0.90 A	Reverse	2,522,000.000 Hz	-09.254 mV	39.4 °C	S

"Coil Polarity" is reversed from now on.

Figure 9: A data table to detect the resonance frequencies for ^{87}Rb using various values of current.

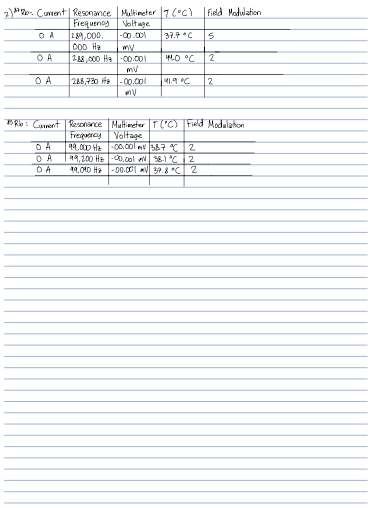

7) ^{85}Rb: Current	Resonance Frequency	Multimeter Voltage	T (°C)	Field Modulation
0 A	289,000.	-00.001	37.7 °C	5
	000. Hz	mV		
0 A	288,000 Hz	-00.001	41.0 °C	2
		mV		
0 A	288,730 Hz	-00.001	41.9 °C	2
		mV		

^{85}Rb: Current	Resonance Frequency	Multimeter Voltage	T (°C)	Field Modulation
0 A	99,000 Hz	-00.001 mV	38.7 °C	2.
0 A	98,220 Hz	-00.001 mV	38.1 °C	2.
0 A	98,090 Hz	-00.001 mV	39.8 °C	2

Figure 10: Data tables to detect the resonance frequencies for ^{85}Rb and ^{87}Rb with no current.

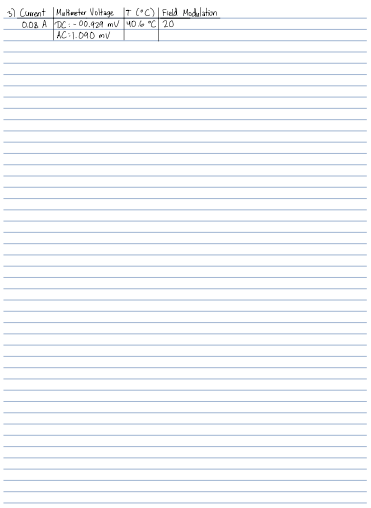

5) Current	Multimeter Voltage	T (°C)	Field Modulation
0.08 A	DC: -00.928 mV	40.6 °C	20
	AC: 1.090 mV		

Figure 11: A Data table to detect the current with zero-field resonance.

7 Data Analysis

The plot of current versus frequency for Rb_{85} and Rb_{87} is given in Figure 12. The frequency for negative current was changed to be negative to allow for a continuous line for both isotopes to be created.

The values for the fitting of the lines in the form of the equation y = mx + b are given in Tables 1-3. The large value of χ^2 and low p-value highlights that the values of uncertainty are lower than the true values.

Isotope	m (MHz/A)	σ_m (MHz/A)
^{85}Rb	2.0289	0.0022
^{87}Rb	3.0440	0.0036

Table 1:

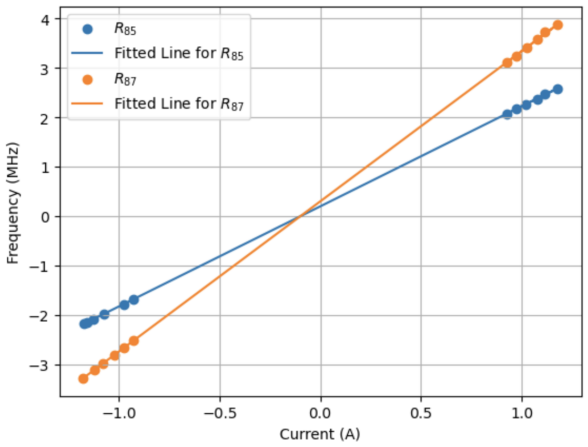

Figure 12: A graph of frequency vs data for Rb_{85} and Rb_{87} for various values of current between 0.90 A to 1.14 A

Isotope	b (MHz)	σ_b (MHz)
^{85}Rb	0.1953	0.0023
^{87}Rb	0.2965	0.0038

Table 2:

Isotope	χ^2	Degrees of Freedom	P
^{85}Rb	106665.7968	10	0
^{87}Rb	1173.5388	10	0

Table 3:

Another component of this experiment is to determine ν_{85}/ν_{87}, I_{85}, and I_{87} through the measured data (1). The equations to find ν_{85}/ν_{87} is given by Equation 13:

$$\frac{\nu_{85}}{\nu_{87}} = \frac{m_{85}}{m_{87}} \tag{13}$$

The values of m_{85} and m_{87} from Table 1 cause ν_{85}/ν_{87} to be equal to 0.66619. However, Equation 13 does not allow for the values of I_{85}/I_{87} to be found. To find the value of I, the slope, m, can be used, as shown in Equation 14, in which N = 135 turns and a = 27.5 cm:

$$m = \frac{(2.799)(0.9 * 10^{-2})(N)}{(2I+1)(a)} \frac{MHz * m}{A} \tag{14}$$

Equation 14 can then be rearranged to solve for I, as shown in Equation 15:

$$I = \frac{(2.799)(0.9 * 10^{-2})(N)}{2ma} \frac{MHz * m}{A} - \frac{1}{2} \tag{15}$$

Furthermore, the values of I calculated from Equation 15, their percent error, and their uncertainty are given in Tables 4 and 5.

Isotope	$I_{experimental}$	$I_{theoretical}$	Percent error
^{85}Rb	2.548	2.5	1.92%
^{87}Rb	1.531	1.5	2.07%

Table 4:

Isotope	σ_I
^{85}Rb	0.00351
^{87}Rb	0.00251

Table 5:

A statistical error that could cause inaccuracy is the uncertainty of line fitting done, as σ_m is 0.0022 MHz/A and 0.0036 MHz/A for ^{85}Rb and ^{87}Rb, respectively. An example of a systematic error that could cause inaccuracy would be the measurement of the resonance symmetry, which is determined by the impression of symmetry (1).

Furthermore, the slope is related to B_H, the Helmholtz field, as shown in Equation 16, in which "i" is the current through the coil. Equation 16 can be rearranged so that B_H can be calculated, as shown in Equation 17 (1).

$$mi = \frac{2.799}{2I+1} B_H * \frac{MHz}{G} \tag{16}$$

$$B_H = \frac{2I+1}{2.799}(mi) * \frac{G}{MHz} \tag{17}$$

The theoretical value of B_H is given by Equation 18:

$$B_H = \frac{0.9 * 10^{-2}}{a}(Ni) * \frac{Gm}{A} \tag{18}$$

The values associated with B_H are given in Tables 6-8.

Isotope	Current (A)	$B_{H_{experimental}}$ (G)
^{85}Rb	0.9254	4.09
^{85}Rb	-0.9257	-4.09
^{87}Rb	0.9243	4.08
^{87}Rb	-0.9254	-4.09

Table 6:

Isotope	Current (A)	$B_{H_{theoretical}}$
^{85}Rb	0.9254	4.09
^{85}Rb	-0.9257	-4.09
^{87}Rb	0.9243	4.08
^{87}Rb	-0.9254	-4.09

Table 7:

Isotope	Current (A)	Percent error (%)
^{85}Rb	0.9254	0
^{85}Rb	-0.9257	0
^{87}Rb	0.9243	0
^{87}Rb	-0.9254	0

Table 8:

A possible source of error when calculating the value of B_H is that the theoretical value involves using the number of turns and radius of the coil, which can fluctuate and thus would impact the results. Additionally, because the calculation of the experimental value of B_H also incorporates slope, due to the slope's uncertainty, the results can be affected as well.

Additionally, the magnitude of the Earth's magnetic field, B_E can be calculated by either measuring the resonance frequency when there is no current being applied or by using the y-intercept of the fitted line to calculate the value of B_E (1). The true value of B_E in Berkeley, California is 0.478 G ("What is the magnetic declination in Berkeley, USA?"). In the first method, the y-intercept and the rearranging of the y-intercept to solve for B_E are given by Equations 19 and 20 (1). The results for the first method are summarized in Table 9.

$$b = \nu = \frac{2.799}{2I+1}(B_E) * \frac{MHz}{G} \tag{19}$$

$$B_E = \frac{\nu(2I+1)}{2.799} * \frac{G}{MHz} \tag{20}$$

Isotope	ν(MHz)	σ_ν (MHz)
^{85}Rb	0.0991	0.0000627
^{87}Rb	0.289	0.000423

Table 9: Finding ν when i = 0 A

Isotope	B_E(G)	σ_{B_E} (G)
^{85}Rb	0.216	0.00840
^{87}Rb	0.419	0.0728

Table 10: Calculating B_E when i = 0 A.

The value of B_E is averaged for both isotopes and is equal to 0.318 G. Additionally, σ_{B_E} is calculated by using propagation of errors and is equal to 0.036 G. Both values and the percent errors are included in Tables 11-12 below.

$B_{E_{Experimental}}$(G)	$B_{E_{Theoretical}}$ (G)
0.318	0.478

Table 11: Finalized value of B_E when i = 0 A

σ_{B_E}	Percent Error
0.036 G	33.47%

Table 12: σ_{B_E} and the percent error when i = 0 A.

In the second method of calculating B_E, 2 values of B_E are received from both isotopes using their intercepts, as shown in Equations 21 and 22 (1). The results of the second method are summarized in Table 10.

$$b = \frac{2.799}{2I+1}(B_E) * \frac{MHz}{G} \tag{21}$$

$$B_E = \frac{2I+1}{2.799}(b) * \frac{G}{MHz} \tag{22}$$

For the second method, the values of B_E are averaged and the errors are propagated, which results

Isotope	B_E(G)	σ_{B_E} (G)
^{85}Rb	0.425	0.0023
^{87}Rb	0.430	0.0038

Table 13: Calculating B_E with the y-intercept of the fitted line of frequency vs current.

in B_E being equal to 0.428 G and σ_{B_E} being equal to 0.00222 G. Both values and the percent errors are included in Tables 13-14 below.

$B_{E_{Experimental}}$ (G)	$B_{E_{Theoretical}}$ (G)
0.428	0.478

Table 14: Finalized value of B_E when using the y-intercept.

σ_{B_E} (G)	Percent error
0.00222	10.46%

Table 15: σ_{B_E} and the percent error when using the y-intercept.

Thus, the method of calculating B_E with the y-intercept of the graph is more accurate, as it has a lower percent error and uncertainty value than the method of calculating B_E by measuring the resonance frequency when i = 0 A.

Additionally, when there is zero field applied to a Helmholtz coil, there is resonance because the Zeeman energy levels become degenerate and thus the atoms can not be pumped into a different energy level (Wolff-Reichert 2009). Figure 13, which is Figure 2 in the reading "A Conceptual Tour of Optical Pumping" by Barbara Wolff-Reichert, displays the increase in light being absorbed by rubidium at zero field.

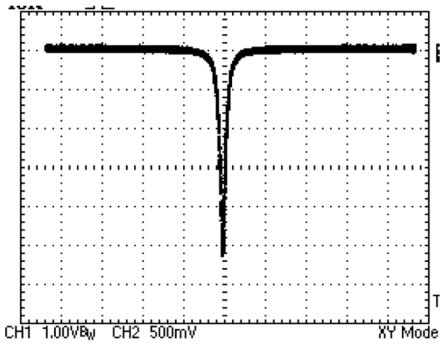

Figure 13: Figure 2 from "A Conceptual Tour of Optical Pumping" by Barbara Wolff-Reichert (6). The x-axis is current, which is related to the magnetic field, and the y-axis is the voltage, which is related to the amount of light absorbed by Rubidium

.

Furthermore, the experimentally-measured value of the pumping time was 0.18 s and the experimentally-measured value of the relaxation time was 0.06 s. As described in the reading "Optical Pumping of Rubidium Vapor" by Emily P. Wang, the pumping time requires values for the rate of transitions to the pumped state and from the pumped

state to a state that is not pumped (P. Wang). The equation to solve for the pumping time is given by Emily P. Wang in "Optical Pumping of Rubidium Vapor" and is written in Equation 23, in which τ is the pumping time, W_u is the rate of transitions to the pumped state, and W_d is the rate of transitions from the pumped state to a state that is not pumped.

$$\tau = \frac{1}{W_u + W_d} \tag{23}$$

8 Conclusions

In conclusion, the "Optical Pumping" lab highlighted the different energy level splitting among isotopes of Rubidium and how polarized light is absorbed by atoms (1). I_{85} was determined to be 2.548 $\pm$ 0.00351 with a percent error of 1.92%. I_{87} was determined to be 1.531 $\pm$ 0.00251 with a percent error of 2.07%. Additionally, the value of B_E was determined to be 0.428 G $\pm$ 0.00222 G with a percent error of 10.46%.

9 Bibliography

(1) Berkeley, University of California. "OPT - Optical Pumping". http://experimentationlab.berkeley.edu/sites/default./files/writeups/OPT.pdf

(2) MIT Department of Physics. "Optical Pumping". 17 February 2011, https://web.mit.edu/8.13/www/JLExperiments/JLExp11.pdf.

(3) P. Wang, Emily. MIT Department of Physics. "Optical Pumping of Ribidium Vapor". https://web.mit.edu/wangfire/pub8.14/oppaper.pdf.

(4) Madison, University of Wisconsin. "Optical Pumping of Ribidium". 6 February 2019, https://www.physics.wisc.edu/courses/home/spring2020/407/experiments/opticalpumping/opticalpumping.pdf.

(5) "What is the magnetic declination in Berkeley, USA?". *Magnetic-Declination*, https://www.magnetic-declination.com/USA/Berkeley/2836070.html. Accessed 12 March 2023.

(6) Wolff-Reichert, Barbara. "A Conceptual Tour of Optical Pumping". 15 July 2009, https://advlabs.aapt.org/tcal/files/BriefIntro_OpticalPumping.pdf.